Enhanced performance of SnO_2 nanowires ethanol sensor by functionalizing with La_2O_3

Nguyen Van Hieu [a,b], Hae-Ryong Kim [a], Byeong-Kwon Ju [c], Jong-Heun Lee [a,*]

[a] Department of Materials Science and Engineering, Korea University, Anam-Dong, Sungbuk-Gu, Seoul 136-713, Republic of Korea
[b] International Training Institute for Materials Science, Hanoi University of Technology, Hanoi, Viet Nam
[c] School of Electrical Engineering, Korea University, Seoul, Republic of Korea

A B S T R A C T

A SnO_2 nanowires (NWs) sensor was coated with a functional La_2O_3 layer by solution deposition and its gas sensing characteristics were compared with those of an uncoated SnO_2 NWs sensor. The responses (R_a/R_g, R_a: resistance in air, R_g: resistance in gas) of an undoped SnO_2 NWs sensor to 100 ppm C_2H_5OH and CH_3COCH_3 were 10.5 and 9.6, respectively, while those to 100 ppm C_3H_8, CO, and H_2 ranged from 3.1 to 3.3. The R_a/R_g values of the La_2O_3-coated SnO_2 NWs to 100 ppm C_2H_5OH and CH_3COCH_3 increased to 57.3 and 34.9, respectively, but there was no significant change in the responses to C_3H_8, CO, and H_2. The ~5.5-fold enhancement in R_a/R_g to C_2H_5OH as well as the selective detection of C_2H_5OH in the interference gases such as C_3H_8, CO, and H_2 was accomplished simultaneously by coating with La_2O_3. In particular, the selective discrimination of C_2H_5OH over CH_3COCH_3, which is a difficult issue on account their similar chemical nature, was possible.

1. Introduction

Quasi-one-dimensional (Q1D) nanostructures of semiconductor metal oxides (SMO) have attracted considerable attention since the successful synthesis of nanobelts of various semiconductor oxides [1]. Significant progress has been made in the synthesis, characterization, and device application of Q1D nanostructures [2]. These structures with a high aspect ratio (i.e., size confinement in two coordinates) offer better crystallinity, higher integration density, and lower power consumption. In addition, they demonstrate superior sensitivity to surface chemical processes due to the large surface-to-volume ratio and small diameter comparable to the Debye length (a measure of the field penetration into the bulk) [3–5]. Although many different Q1D nanostructures of SMO such as SnO_2, ZnO, In_2O_3, and TiO_2 have been investigated for their gas sensing properties, researchers have paid greater attention to SnO_2 nanowires (NWs)-based sensors because their counterparts such as a thick film, porous pellets and thin films are versatile in being able to sense a variety of gases [6–8] and are commercially available. Thus far, the excellent sensing properties of SnO_2 Q1D nanostructures have been applied to the detection of various gases such as C_2H_5OH [9–11], CO [12], NO_2 [11,13], O_2 [12], and O_3 [13].

The selectivity and sensitivity of SnO_2 NWs sensors can be enhanced either by doping with other oxide materials [14–16] or by functionalizing with catalytically active materials [17–19]. Oxide materials are usually doped by the thermal evaporation of a mixed source material [14–16]. Noble catalyst materials are generally deposited by vapor deposition [17,18] or sputtering [19] next to the growth of SnO_2 NWs. A source material for doping with an appropriate vapor pressure is indispensable for the thermal evaporation of mixed materials and there is a limitation in the precise control of the dopant concentration. Moreover, the deposition of catalyst materials after the growth of NWs is relative complex and not cost-effective. Accordingly, a convenient approach to form a functional layer on SnO_2 NWs is essential for enhancing the selectivity and sensitivity, as well as for achieving a simple process at low cost.

It is remarkable that most of the studies on SnO_2 NWs sensors for detecting C_2H_5OH to date are based on the SnO_2 NWs [9–11]. However, there are no reports on the enhancement of sensitivity and selectivity through functionalization with catalytically active oxide materials. This paper suggests a convenient solution deposition route for functionalizing SnO_2 NWs sensors with La_2O_3. La_2O_3 was selected as the catalytically active material because it has been reported to be a promising promoter for SnO_2-based C_2H_5OH sensors [20,21]. Although the role of La_2O_3 in enhancing the sensitivity to C_2H_5OH is relatively well known, the effect of La_2O_3 doping on the sensing

of other gases and the selective detection of a specific gas is unclear.

In this study, SnO_2 NWs were grown by thermal evaporation and the SnO_2 NWs sensors were functionalized with La_2O_3 by dropping a $La(NO_3)_3$ solution at different concentrations. The sensing characteristics to C_2H_5OH, CH_3COCH_3, C_3H_8, CO, and H_2 of the SnO_2 NWs sensors without and with the functional La_2O_3 layer were compared. The main focus was placed on the role of La_2O_3 in enhancing the sensitivity to C_2H_5OH, the selective detection of C_2H_5OH in the presence of interference gases such as CH_3COCH_3, C_3H_8, CO and H_2, and the gas response time.

2. Experimental

2.1. Growth of SnO₂ nanowires

The schematic diagram of experimental setup for the growth of SnO_2 NW was shown in Fig. 1. The SnO_2 NWs were grown in a quartz tube located in a horizontal furnace with a sharp temperature gradient. Both ends of the quartz tube were sealed with rubber O-rings. The ultimate vacuum for this configuration was $\sim 2 \times 10^{-3}$ torr. The carrier gas-line (Ar) and O_2 gas-line were connected to the left-end of a quartz tube and their flow rate was modulated by a digital mass-flow-control system. The right end of the quartz tube was connected to a rotary pump through a needle valve in order to maintain a desired pressure in the tube. High-purity SnO_2 powder (Merck, 99.9%) was placed in one end of an alumina boat as an evaporation source. In the same boat, an alumina substrate with a previously deposited Au catalyst layer (thinness: ~ 10 nm) was placed approximately 2–3 cm from the source along the direction of gas flow. The entire boat was covered with an alumina plate. A small opening was left to allow the gas to flow into the assembly. The complete unit was placed into the quartz tube for the NWs growth. The growth process was divided into two steps. Initially, the quartz tube was evacuated to 10^{-2} torr and purged several times with Ar gas. Subsequently, the furnace temperature was increased to 960 °C for 30 min. During this step, only Ar gas was introduced into the furnace at a flow rate of 50 sccm and the pressure was maintained in the range of 100–200 torr. When the temperature reached 960 °C, oxygen gas was added to the quartz tube at a flow rate of 0.5 sccm, and the process was maintained for 2 h during the growth of the SnO_2 NWs. The SnO_2 NWs were analyzed by scanning electron microscopy (SEM, Hitachi S-4300), transmission electron microscopy (TEM, FEI Tecnai 20), and X-ray diffraction (XRD, Rigaku D/MAX-2500V/PC).
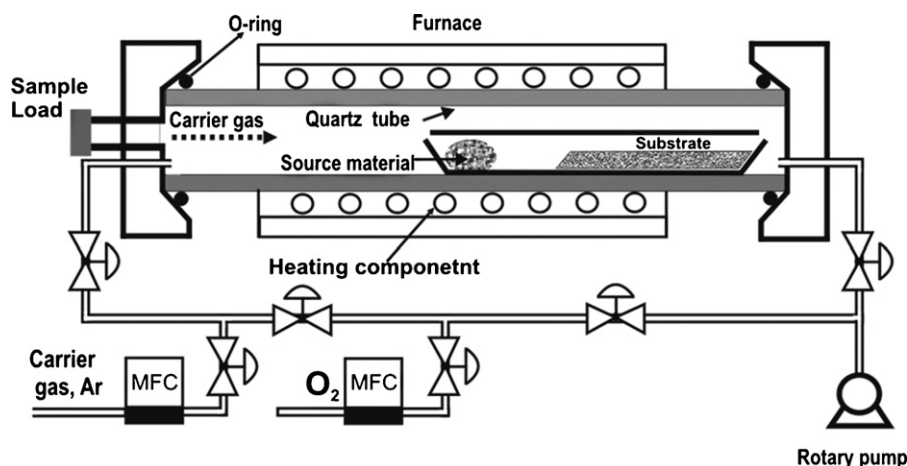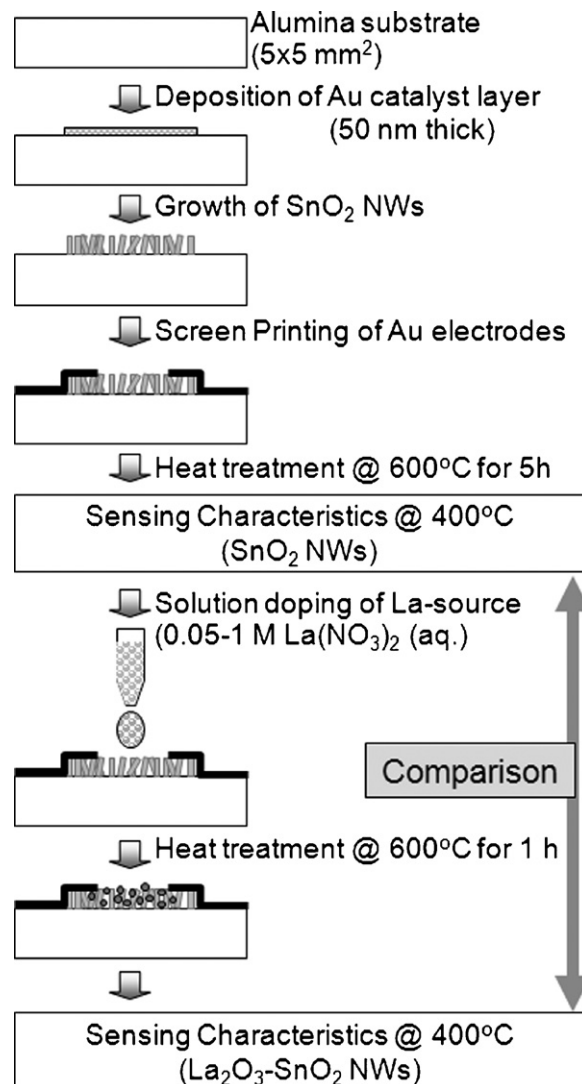

Fig. 2. Schematic diagram of the sensor configuration and experimental procedures.

2.2. Sensor fabrication and characterization

Fig. 2 shows a schematic diagram of sensor fabrication and characterization. Comb-shape Au electrodes were screen printed on the

Fig. 1. Experimental setup for the growth of SnO_2 nanowires.

top of the SnO_2 NWs grown on an alumina substrate and subsequently heat-treated at 600 °C for 5 h. The sensor was installed in a quartz tube and the furnace temperature was stabilized at a constant sensing temperature (400 °C). The gas concentration was controlled by changing the mixing ratio of the parent gases (200 ppm C_2H_5OH, 100 ppm CH_3COCH_3, 200 ppm C_3H_8, 100 ppm CO, and 200 ppm H_2 all in air balance) and dry synthetic air. A flow-through technique with a constant flow rate (500 ml/min) was used. The gas response ($S = R_a/R_g$) was measured at 400 °C by comparing the resistance of the sensor in high-purity air (R_a) with that in the target gases (R_g). The electrical resistance of the sensor was monitored using a Picroammeter/Voltage Source (Keithley 6487) interfaced with a computer.

The effect of La_2O_3 doping on the sensitivity and selectivity of the SnO_2 sensor was examined by placing a droplet of 0.05, 0.5, and 1 M $La(NO_3)_3$ aqueous solutions (volume = ~0.87 μl) onto the SnO_2 NW sensors using a micropipette (DV10, High Tech Labs). The sensor was heat-treated at 600 °C for 1 h to remove any moisture and to convert the $La(NO_3)_3$ into La_2O_3. The gas sensing characteristics of the La_2O_3-doped SnO_2 NWs sensor were measured under identical experimental conditions used for the pure SnO_2 NWs sensor. The sensing characteristics before and after La_2O_3 doping were compared.

3. Results and discussion

3.1. Microstructural characterizations

Fig. 3 shows the morphology of the as-prepared SnO_2 NWs. Uniform SnO_2 NWs with homogeneous entanglement were produced on a large area (1 cm × 5 cm). The diameter of the SnO_2 NWs ranged from 50 to 100 nm and the lengths ranged from several tens to hundreds of micrometers. All the NWs were smooth and uniform along the fiber axis. SnO_2 NWs with a catalyst particle on its tip (Fig. 3(c)) were observed. EDS analysis (not shown) revealed

that the catalyst particle was composed of Au, Sn, and O, which indicates that the SnO_2 NWs were grown via a vapor–liquid–solid (VLS) mechanism [1–3,11,13]. The morphology of SnO_2 NWs functionalized with La_2O_3 using a 0.5 M $La(NO_3)_3$ solution was shown in Fig. 4. In the low magnification image (Fig. 4(a)), it was difficult to observe the La_2O_3-related phase. However, the second phases could be frequently found on the surface of SnO_2 NWs in the high-magnification SEM and TEM images (see arrows in Fig. 4 (b–d)), which were identified not as catalyst particles but as La_2O_3-containing phase according to EDS analysis.

The XRD patterns of the as-synthesized SnO_2 NWs (Fig. 5) were indexed to the tetragonal rutile structure, which agrees well with JCPDS 77-0450. According to the JCPDS file, the intensity ratio between the (1 1 0) and (1 0 1) peaks is 1000/767. However, the intensity ratio between the (1 1 0) and (1 0 1) peaks in Fig. 5 was 653/1000, which suggests a preferred orientation.

3.2. Gas sensing properties

Fig. 6 shows the responses to C_2H_5OH, CH_3COCH_3, C_3H_8, CO, and H_2 of the SnO_2 NWs sensor before and after La_2O_3 doping using a 0.5 M $La(NO_3)_3$ aqueous solution. All the gas concentrations were fixed to 100 ppm for comparison. In the undoped SnO_2 NWs sensor, the responses ($S = R_a/R_g$) to C_2H_5OH and CH_3COCH_3 were 10.5 and 9.6, respectively. These responses are higher than those for C_3H_8 ($S = 3.3$), CO ($S = 3.3$), and H_2 gases ($S = 3.1$). Therefore, the selective sensing of C_2H_5OH and CH_3COCH_3 in the presence of C_3H_8, CO, and H_2 is possible. The responses to C_2H_5OH and CH_3COCH_3 were increased to 57.3 and 34.9 by doping with La_2O_3, respectively, which are significantly higher than those of the pure SnO_2 NWs sensor. In contrast, the responses of the La_2O_3-doped SnO_2 NWs to C_3H_8, CO and H_2 were 3.8, 3.5, and 2.8, respectively, which are similar to the undoped SnO_2 NWs sensor.

The level of La_2O_3 doping was controlled by varying the concentrations of the $La(NO_3)_3$ aqueous solution from 0.05 to 1 M. The
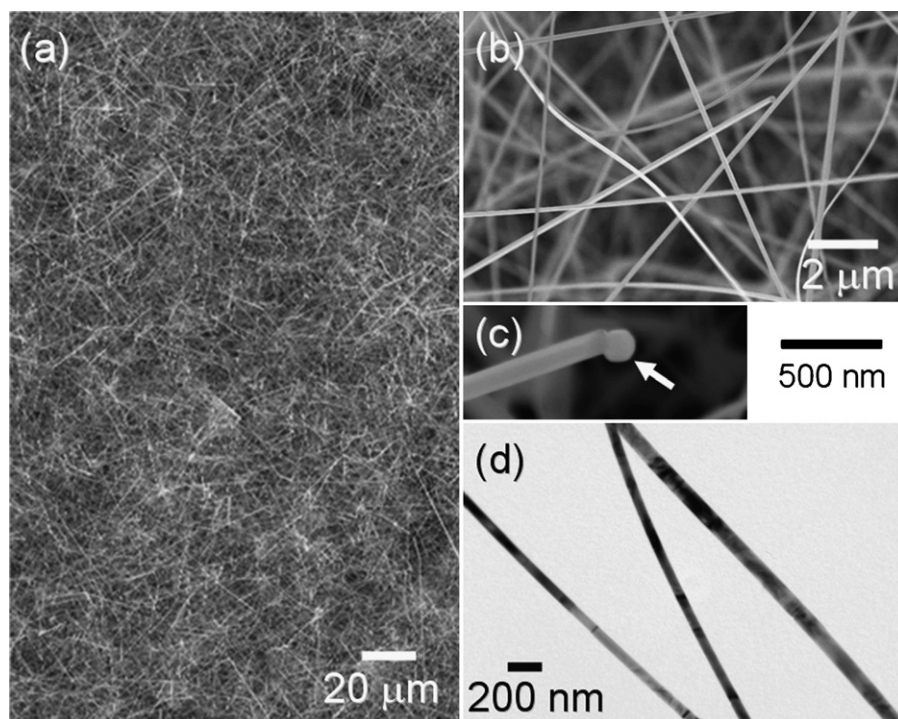

Fig. 3. SEM and TEM images of SnO_2 nanowires: (a) low resolution SEM image; (b) high resolution SEM image; (c) high resolution SEM image showing catalytic particle on top of SnO_2 nanowire; and (d) high resolution TEM image.
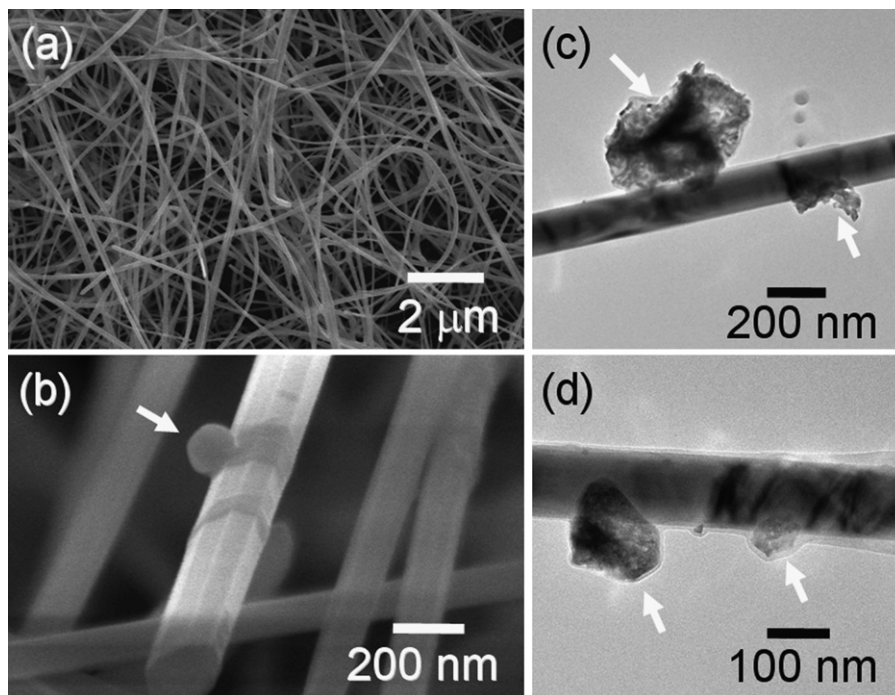
Fig. 4. SEM and TEM images of SnO_2 nanowires functionalized with La_2O_3 using a 0.5 M $La(NO_3)_3$ solution after heat-treatment at 600 °C for 5 h: (a) low resolution SEM image; (b) high resolution SEM image; and (c), (d) high resolution TEM images.

gas sensing characteristics of the sensors before and after La_2O_3 doping were compared using a polar plot (Fig. 7). Three undoped SnO_2 NW sensors showed similar sensing characteristics (Fig. 7, empty circles in left three diagrams), which confirmed the reproducibility of the SnO_2 NWs sensors. After doping with La_2O_3, the responses to C_2H_5OH and CH_3COCH_3 increased 2–6 times while those to C_3H_8, CO, and H_2 remain approximately the same. This indicates that La_2O_3 doping enhances the responses to C_2H_5OH and CH_3COCH_3.

In order to quantify the effect of La_2O_3 on the gas responses, the ratio between the responses to a specific gas before and after La_2O_3 doping ($RR_{gas} = S_{gas}(La_2O_3–SnO_2)/S_{gas}(SnO_2)$) were calculated and plotted in right three diagrams, as shown in Fig. 7. For example, $RR_{ethanol}$ is the ratio between the response to 100 ppm C_2H_5OH of the La_2O_3-doped SnO_2 NWs and that of the undoped SnO_2 NWs. When doped with La_2O_3 using a 0.05 M $La(NO_3)_3$ solution, the $RR_{ethanol}$ and $RR_{acetone}$ values were 3.7 and 3.2, respectively (Fig. 7 right upper). It should be noted that the $RR_{ethanol}$ value was increased to 5.5 by doping La_2O_3 using a 0.5 M $La(NO_3)_3$ solution while the $RR_{acetone}$ value was increased to 3.6 (Fig. 7 right mid-

dle). A further increase in the La_2O_3 concentration decreased the $RR_{ethanol}$ and $RR_{acetone}$ values to 2.6 and 1.9, respectively (Fig. 7 right below). This shows that the concentration of La_2O_3 should be optimized in order to maximize the sensing responses to C_2H_5OH and CH_3COCH_3.

The decomposition of C_2H_5OH at high temperature is dependent upon the acid–base properties of the oxide catalyst used [12].

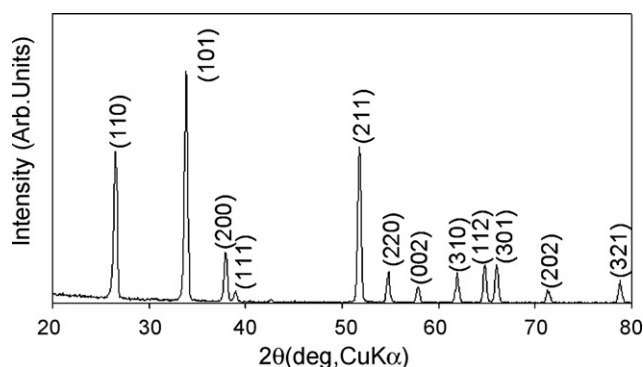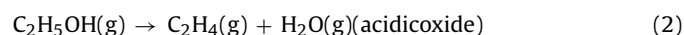$$C_2H_5OH(g) \rightarrow CH_3CHO(g) + H_2(g) (basic oxide) \tag{1}$$

$$C_2H_5OH(g) \rightarrow C_2H_4(g) + H_2O(g) (acidic oxide) \tag{2}$$

Fig. 6. Gas responses to 100 ppm of C_2H_5OH, CH_3COCH_3, C_3H_8, CO, and H_2 at 400 °C of (a) undoped SnO_2 nanowires and (b) La_2O_3-doped SnO_2 nanowires using 0.5 M $La(NO_3)_3$ solution.
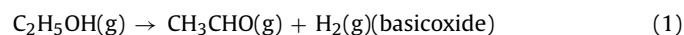
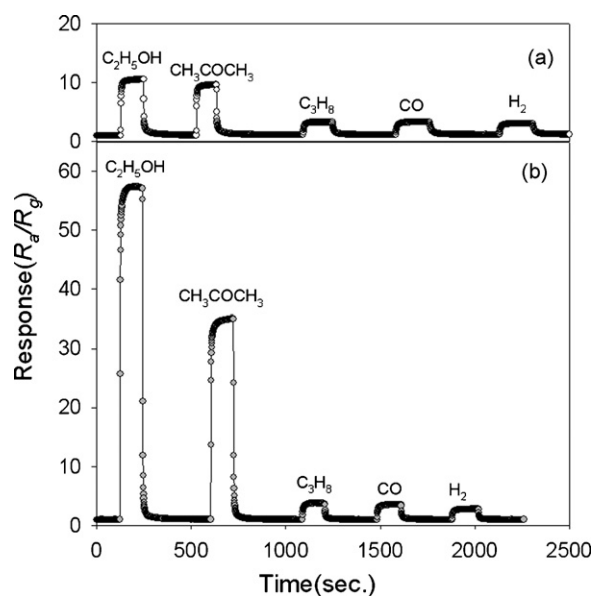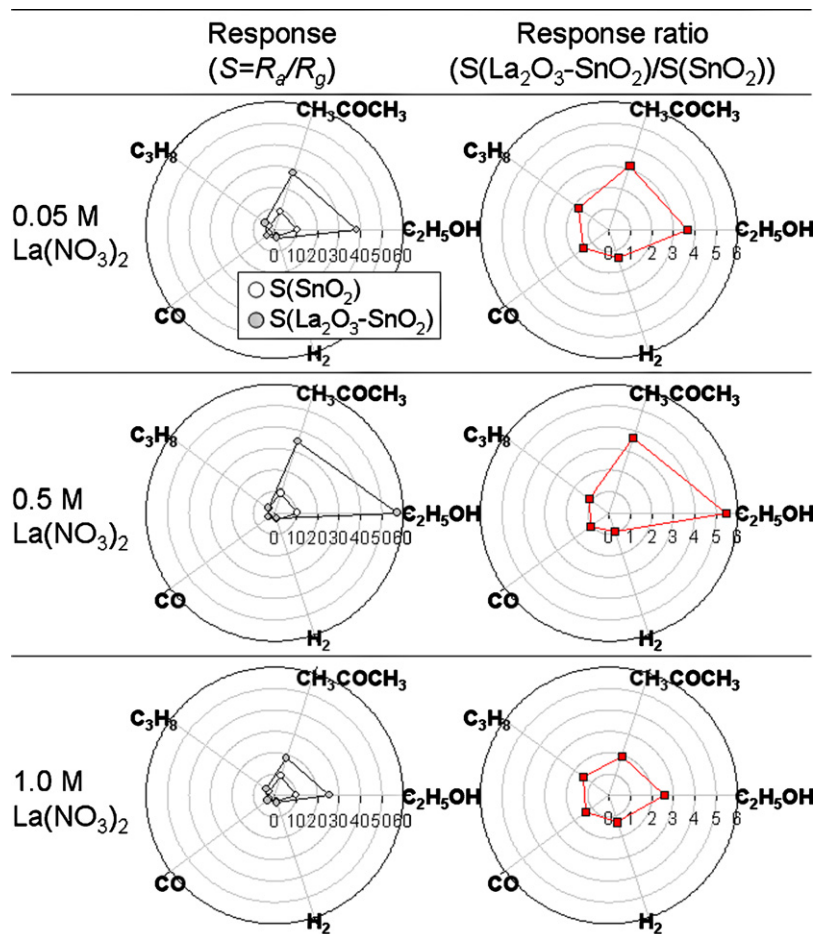**Fig. 5.** X-ray diffraction pattern of the undoped SnO_2 nanowires.

Fig. 7. Polar plots of the gas responses to C_2H_5OH, CH_3COCH_3, C_3H_8, CO, and H_2 before and after doping with La_2O_3 using 0.05, 0.5, and 1.0 M $La(NO_3)_3$ solutions, and the ratio between the responses to a specific gas before and after La_2O_3 doping. Gas sensing characteristics were measured at 400 °C, and the concentration of all gases was fixed to 100 ppm.

Jinkawa et al. [20] reported that the sensitivity to C_2H_5OH is increased 10–40 times by the addition of basic oxides such as Cs_2O, La_2O_3, and Gd_2O_3. $CH_3CHO(g) + H_2(g)$ in a basic oxide induces a larger increase in conductance than C_2H_4 (g) in an acidic oxide. Therefore, the 5.5-fold increase in $S_{ethanol}$ by La_2O_3 doping can be attributed to the promotion of reaction (1).

The doping of different La_2O_3 concentrations increased the $RR_{ethanol}$ value more than the $RR_{acetone}$ value. The $S_{ethanol}/S_{acetone}$ ratio, which is the degree of selective detection to C_2H_5OH in the presence of CH_3COCH_3, was ~1.10 for the undoped SnO_2 NW sensors. In this circumstance, discrimination between C_2H_5OH and CH_3COCH_3 is almost impossible. Indeed, the $S_{ethanol}$ value in the most oxide semiconductor gas sensors was reported to be similar to the $S_{acetone}$ value [21–27]. The reason for this can be found from the similar reaction intermediates, $CH_3CHO(g)$, which is formed by the decompositions of C_2H_5OH [12] and CH_3COCH_3 [28].

In this study, the $S_{ethanol}/S_{acetone}$ ratio increased to 1.38, 1.64, and 1.39 when doped with La_2O_3 using the 0.05, 0.5, and 1 M $La(NO_3)_3$ solutions, respectively. This means that doping with La_2O_3 promotes the sensing reaction to C_2H_5OH more than to CH_3COCH_3. Accordingly, La_2O_3 doping not only enhances the response to C_2H_5OH to a great extent but also enables the selective detection of C_2H_5OH in the presence of CH_3COCH_3, which is a challenging issue.

The dynamic response transients were obtained for the undoped and La_2O_3-functionalized SnO_2 NWs sensors (Fig. 8). The 90% response time for gas exposure ($t_{90\%(air-to-gas)}$) and that for recovery ($t_{90\%(gas-to-air)}$) were calculated from the resistance–time data

shown in Figs. 6 and 8 and are summarized in Table 1. In the undoped SnO_2 NWs sensor, the $t_{90\%(air-to-gas)}$ values in the sensing of C_2H_5OH and CH_3COCH_3 ranged from 2 to 4 s, while the $t_{90\%(gas-to-air)}$ value ranged from 98 to 136 s. The $t_{90\%(air-to-gas)}$ values in the sensing of C_3H_8, CO, and H_2 were 9–13 s while the $t_{90\%(gas-to-air)}$ value decreased to 62–65 s. This shows that the sensing mechanisms of C_2H_5OH and CH_3COCH_3 are different from those of C_3H_8, CO, and H_2. Note that the $t_{90\%(air-to-gas)}$ values in the range of 2–4 s in sensing C_2H_5OH and CH_3COCH_3 and those in the range of 9–13 s in sensing C_3H_8, CO, and H_2 are quite short considering that the sensor response times in the most of the literature range from 60 to 120 s [10,29,30]. This can be explained by the rapid in-diffusion of gas towards the sensing surface due to the less-agglomerated network structure of NWs. When doped with La_2O_3, both the $t_{90\%(air-to-gas)}$ values and $t_{90\%(gas-to-air)}$ values were shortened compared with those of the undoped SnO_2 NWs sensors. Therefore, doping with La_2O_3 is a promising approach for enhancing the sensitivity and selectivity to C_2H_5OH without deteriorating the rapid sensor response.

The sensor resistance in air (R_a) was increased by doping with La_2O_3, as shown in Fig. 8. Kugishima et al. [31] reported that the R_a value of undoped SnO_2 at 400 °C is increased by ~1.5 orders of magnitude by doping with 0.5 wt% La_2O_3. They [32] also reported that the R_a value of Sb-doped SnO_2 at 400 °C is increased by up to ~5 orders of magnitude with increasing La_2O_3 doping concentrations from 0.5 to 5 wt%. A further increase in the La_2O_3 concentration to 7 wt% decreased the R_a value. It is interesting that the response

Table 1
The 90% response time for the gas exposure ($t_{90\%(\text{air-to-gas})}$) and that for recovery ($t_{90\%(\text{gas-to-air})}$) (measured at 400 °C)

Gas	SnO$_2$ NWs		La$_2$O$_3$–SnO$_2$ NWs	
	$t_{90\%(\text{air-to-gas})}$ (s)	$t_{90\%(\text{gas-to-air})}$ (s)	$t_{90\%(\text{air-to-gas})}$ (s)	$t_{90\%(\text{gas-to-air})}$ (s)
C$_2$H$_5$OH 10 ppm	4	98	1	88
C$_2$H$_5$OH 50 ppm	3	114	1	81
C$_2$H$_5$OH 100 ppm	2	136	1	110
CH$_3$COCH$_3$ 100 ppm	2	127	1	78
C$_3$H$_8$ 100 ppm	9	65	6	47
CO 100 ppm	12	65	7	54
H$_2$ 100 ppm	13	62	8	40

to 20 ppm ethylene oxide (C$_2$H$_4$O) increases until 5 wt% La$_2$O$_3$ and then decreases at 7 wt% La$_2$O$_3$. This reflects that the response (R_a/R_g) is related to the R_a value and can be understood from the finding that the relative decrease of sensor resistance becomes more evident at the higher R_a when a constant amount of electrons is supplied by the gas sensing reaction at the surface. The R_a values for the three undoped SnO$_2$ NWs sensors were 11.7, 14.1, and 8.5 MΩ, respectively. These values increased to 66.8, 415.4, and 181.0 MΩ after doping with La$_2$O$_3$ using 0.05, 0.5, and 1.0 M La(NO$_3$)$_3$ aqueous solutions, respectively. These correspond to a 7.8-, 29.6-, and 15.4-fold increase in R_a, respectively. Although further systematic studies will be necessary, La$_2$O$_3$ appears to play a dual roles as an acceptor and a catalytic promoter and the highest enhancement of the C$_2$H$_5$OH response with the La$_2$O$_3$ coating using a 0.5 M La(NO$_3$)$_3$ aqueous solution can be understood in a similar viewpoint. The relative contributions between the catalytic activation and the increase in R_a by doping with La$_2$O$_3$ need to be studied in order to better understand the detailed C$_2$H$_5$OH sensing mechanism of La$_2$O$_3$-doped SnO$_2$ sensors.

One of important applications for a C$_2$H$_5$OH sensor is the screening of inebriated drivers. Under heavy traffic conditions, the ambient concentrations of CO can increase up to 100 ppm as a result of emission from gasoline engines [33]. In addition, CH$_3$COCH$_3$
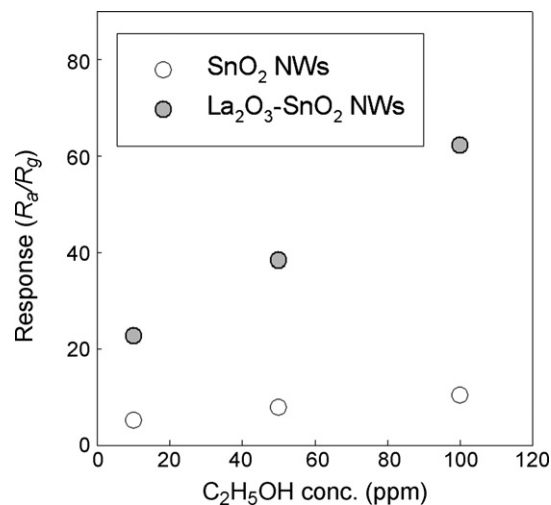
Fig. 9. Response to 10–100 ppm C$_2$H$_5$OH of the SnO$_2$ NWs sensors before and after the doping with La$_2$O$_3$ using a 0.5 M La(NO$_3$)$_3$ solution (measured at 400°C).

vapor can be contained in the expiration from a diabetes patient [34], which can reach concentrations up to 300 ppm in the case of an aceto-acidotic coma related to diabetes mellitus [35]. In this respect, SnO$_2$ NWs functionalized with La$_2$O$_3$ using a 0.5 M La(NO$_3$)$_3$ solution can be used to detect C$_2$H$_5$OH selectively in the presence of interfering gases such as CO and CH$_3$COCH$_3$ although the cross-sensitivity to CH$_3$COCH$_3$ should be decreased further.

Fig. 9 shows the responses to 10–100 ppm C$_2$H$_5$OH of undoped and La$_2$O$_3$-doped SnO$_2$ NWs sensors. The response to 10 ppm increased from 5.1 to 22.7 and that to 100 ppm increased from 22.7 to 62. This is higher than SnO$_2$-nanobelts ($\Delta G/G = 41.2$ for 250 ppm C$_2$H$_5$OH) [10], Sb-doped SnO$_2$ NWs ($R_a/R_g = \sim 3$ for 800 ppm C$_2$H$_5$OH) [14], indium-doped SnO$_2$ NWs ($R_a/R_g = \sim 7$ for 50 ppm C$_2$H$_5$OH) [15], ZnO NWs ($R_a/R_g = \sim 15$ for 100 ppm C$_2$H$_5$OH) [36], ZnSnO$_3$ NWs ($R_a/R_g = \sim 18$ for 100 ppm C$_2$H$_5$OH) [37], In$_2$O$_3$ NWs ($R_a/R_g = \sim 2$ for 100 ppm C$_2$H$_5$OH) [38], and V$_2$O$_5$ NWs ($R_a/R_g = \sim 2$ for 200 ppm C$_2$H$_5$OH) [39], and is comparable to the results of other SnO$_2$-nanobelts ($\Delta G/G = 25$ for 10 ppm C$_2$H$_5$OH) [11]. This clearly shows that these SnO$_2$ NWs with a La$_2$O$_3$ functional layer have the potential to achieve ultra-high gas sensitivity.

Finally, it should be noted that the sensor fabrication platform in this study is quite simple and inexpensive. A coating of a functional La$_2$O$_3$ layer by solution deposition and the control of the doping concentration is very convenient compared with the element doping in the stage of NWs growth. This suggests that a solution-based coating of a functional layer on SnO$_2$ NWs is a powerful approach for accomplishing high sensitivity and selectivity without deteriorating the gas response time. This method can be easily used to develop semiconducting NWs sensors functionalized with different catalyst materials such as Pd, Pt, or Au, which has great potential in the sensing of multiple gases using a sensor array.
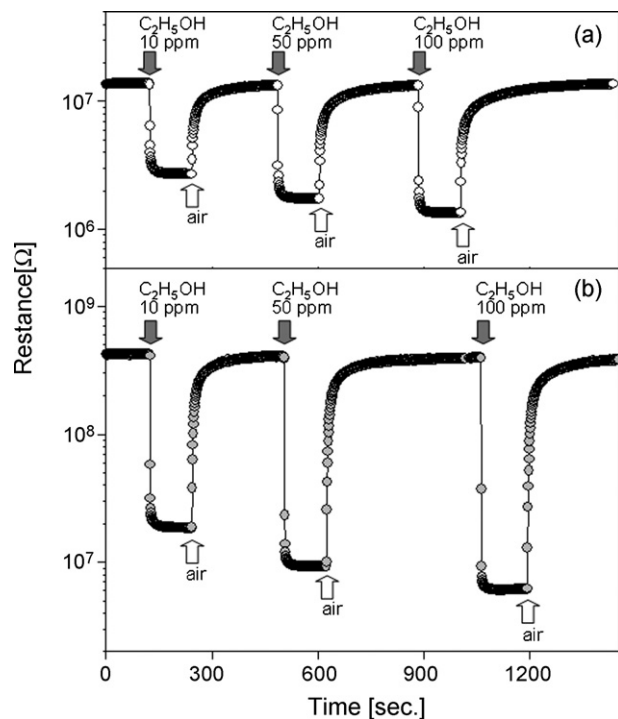
Fig. 8. Response transients to 10–100 ppm C$_2$H$_5$OH of (a) undoped SnO$_2$ nanowires sensor and (b) La$_2$O$_3$-doped SnO$_2$ nanowires sensor using a 0.5 M La(NO$_3$)$_3$ solution (measured at 400 °C).

4. Conclusion

A La_2O_3 layer was coated on SnO_2 nanowires gas sensors by the deposition of $La(NO_3)_3$ aqueous solutions, and its effect on the gas sensing characteristics to C_2H_5OH, CH_3COCH_3, C_3H_8, CO and H_2 were investigated. The La_2O_3 coating using a 0.5 M La $(NO_3)_3$ aqueous solution greatly increased the responses to C_2H_5OH ($\sim$5.5 times) and CH_3COCH_3 ($\sim$3.6 times) but did not vary the responses to C_3H_8, CO, and H_2. The discrimination between C_2H_5OH and CH_3COCH_3, which is a challenging issue due to their similar chemical nature, was accomplished by the more active promotion of C_2H_5OH sensing over CH_3COCH_3 sensing. The deposition of La_2O_3 via the solution route, suggested in this study, provides an effective and convenient route for accomplishing both high sensitivity and high selectivity to C_2H_5OH without deteriorating the gas response kinetics.

Acknowledgements

References

[1] Z.W. Pan, Z.R. Dai, Z.L. Wang, Nanobelts of semiconducting oxide, Science 291 (2001) 1947–1949.
[2] J.G. Lu, P. Chang, Z. Fan, Quasi-one-dimensional metal oxide materials—synthesis, properties and applications, Mater. Sci. Eng. R 52 (2006) 49–91.
[3] E. Comini, Metal oxide nano-crystals for gas sensing, Anal. Chim. Acta 568 (2006) 28–40.
[4] A. Kolmakov, M. Moskovits, Chemical sensing and catalysis by one-dimensionalmetal-oxide nanostructures, Ann. Rev. Mater. Res. 34 (2004) 150–180.
[5] X.-J. Huang, Y.-K. Choi, Chemical sensors based on nanostructured materials, Sens. Actuators B 122 (2006) 659–671.
[6] N. Yamazoe, Toward innovations of gas sensor technology, Sens. Actuators B 108 (2005) 2–14 (review).
[7] Y. Shimizu, M. Egashira, Basic aspects and challenges of semiconductor gas sensors, MRS Bull. 24 (1999) 18–24.
[8] C.C. Wang, S.A. Akbar, M.J. Madou, Ceramic based resistive sensors, J. Electroceram. 2 (4) (1998) 273–282.
[9] Y.J. Chen, X.Y. Xue, Y.G. Wang, T.H. Wanga, Synthesis and ethanol sensing characteristics of single crystalline SnO_2 nanorods, Appl. Phys. Lett. 87 (23351) (2005) 01–03.
[10] E. Comini, G. Faglia, G. Sberveglieri, Z. Pan, Z.L. Wang, Stable and highly sensitive gas sensors based on semiconducting oxide nanobelts, Appl. Phys. Lett. 81 (2002) 1869–1871.
[11] E. Comini, G. Faglia, G. Sberveglieri, D. Calestani, L. Zanotti, M. Zha, Tin oxide nanobelts electrical and sensing properties, Sens. Actuators B 111–112 (2005) 2–6.
[12] A. Kolmakov, Y. Zhang, G. Cheng, M. Moskovits, Detection of CO and O_2 using tin oxide nanowires, Adv. Mater. 15 (2003) 997–1000.
[13] G. Sberveglieri, C. Baratto, E. Comini, G. Faglia, M. Ferroni, A. Ponzoni, A. Vomiero, Synthesis and characterization of semiconducting nanowires for gas sensing, Sens. Actuators B 121 (2007) 208–213.
[14] Q. Wan, T.H. Wang, Single-crystalline Sb-doped SnO_2 nanowires: synthesis and gas sensor application, Chem. Commun. (2005) 3841–3843.
[15] X.Y. Xue, Y.J. Chen, Y.G. Liu, S.L. Shi, Y.G. Wang, T.H. Wang, Synthesis and ethanol sensing properties of indium-doped tin oxide nanowires, Appl. Phys. Lett. 88 (2006) 201907.
[16] N.S. Ramgir, I.S. Mulla, K.P. Vijayamohanan, A room temperature nitric oxide sensor actualized from Ru-doped SnO_2 nanowires, Sens. Actuators B 107 (2005) 708–715.
[17] A. Kolmakov, D.O. Klenov, Y. Lilach, S. Stemmer, M. Moskovits, Enhanced gas sensing by individual SnO_2 nanowires and nanobelts functionalized with Pd catalyst particles, Nano Lett. 5 (2005) 667–673.
[18] L.H. Qian, K. Wang, Y. Li, H.T. Fang, Q.H. Lu, X.L. Ma, CO sensor based on Au-decorated SnO_2 nanobelt, Mater. Chem. Phys. 100 (2006) 82–84.
[19] H.T. Wang, B.S. Kang, R. Ren, L.C. Tien, P.W. Sadik, D.P. Norton, S.J. Pearton, Hydrogen-selective sensing at room temperature with ZnO nanorods, Appl. Phys. Lett. 86 (2005) 243503.
[20] T. Jinkawa, G. Sakai, J. Tamaki, N. Miura, N. Yamazoe, Relationship between ethanol gas sensitivity and surface catalytic property of tin oxide sensors modified with acidic or basic oxides, J. Mol. Catal. A Chem. 155 (2000) 193–200.
[21] I. Stambolova, K. Konstantinov, S. Vassilev, P. Peshev, Ts. Tsacheva, Lanthanum doped SnO_2 and ZnO thin films sensitive to ethanol and humidity, Mater. Chem. Phys. 63 (2000) 104–108.
[22] B.L. Zhu, C.S. Xie, W.Y. Wang, K.J. Huang, J.H. Hu, Improvement in gas sensitivity of ZnO thick film to volatile organic compounds (VOCs) by adding TiO_2, Mater. Lett. 58 (2004) 624–629.
[23] H. Gong, Y.J. Wang, S.C. Teo, L. Huang, Interaction between thin-film tin oxide gas sensor and five organic vapors, Sens. Actuators B 54 (1999) 232–235.
[24] X. Li, G. Zhang, F. Cheng, B. Guo, J. Chen, Synthesis characterization and gas-sensor application of WO_3 nanocuboids, J. Electrochem. Soc. 153 (2006) H133–H137.
[25] Z. Jing, Y. Wang, S. Wu, Preparation and gas sensing properties of pure and doped γ-Fe_2O_3 by an anhydrous solvent method, Sens. Actuators B 113 (2006) 177–181.
[26] Y. Jiang, W. Song, C. Xie, A. Wang, D. Zeng, M. Hu, Electrical conductivity and gas sensitivity to VOCs of V-doped ZnFe_2O_4 nanoparticles, Mater. Lett. 60 (2006) 1374–1378.
[27] Z. Jie, H. Li-Hua, G. Shan, Z. Hui, Z. Jing-Gui, Alcohols and acetone sensing properties of SnO_2 thin films deposited by dip-coating, Sens. Actuators B 115 (2006) 460–464.
[28] T. Tsuboi, K. Ishii, S. Tamura, Thermal oxidation of acetone behind reflected shock wave, in: Proceedings of the 17th International Colloquium on the Dynamics of Explosions and Reactive Systems, Heidelberg, Germany, July 25–30, 1999.
[29] Y.-K. Jun, H.-S. Kim, J.-H. Lee, S.-H. Hong, CO sensing performance in micro-arc oxidized TiO_2 films for air quality control, Sens. Actuators B 120 (2006) 69–73.
[30] K. Galatsis, Y.X. Li, W. Wlodarski, E. Comini, G. Faglia, G. Sberveglieri, Semiconductor MoO_3–TiO_2 thin film gas sensors, Sens. Actuators B 77 (2001) 472–477.
[31] M. Kugishima, G. Sakai, K. Shimanoe, N. Yamazoe, Development of SnO_2-based gas sensor sensitive to dilute ethylene oxide in air, Sens. Actuators B 108 (2005) 130–135.
[32] M. Kugishima, K. Shimanoe, N. Yamazoe, C_2H_4O sensing properties for thick film sensor using La_2O_3-modified SnO_2, Sens. Actuators B 118 (2006) 171–176.
[33] H. Nakagawa, S. Okazaki, S. Asakura, K. Fukuda, H. Akimoto, S. Takahashi, S. Shigemori, An automated car ventilation system, Sens. Actuators B 65 (2000) 133–137.
[34] S.V. Ryabsev, A.V. Shaposhnick, A.N. Lukin, E.P. Domashevskaya, Application of semiconductor gas sensors for medical diagnostics, Sens. Actuators B 59 (1999) 26–29.
[35] M. Fleischer, E. Simon, E. Rumpel, H. Ulmer, M. Harbeck, M. Wandel, C. Fietzek, U. Weimar, H. Meixner, Detection of volatile compounds correlated to human diseases trough breath analysis with chemical sensors, Sens. Actuators B 83 (2002) 245–249.
[36] Q. Wan, Q.H. Li, Y.J. Chen, T.H. Wang, X.L. He, J.P. Li, C.L. Lin, Fabrication and ethanol sensing characteristics of ZnO nanowire gas sensors, Appl. Phys. Lett. 84 (2004) 3654–3656.
[37] X.Y. Xue, Y.J. Chen, Y.G. Wang, T.H. Wang, Synthesis and ethanol sensing properties of ZnSnO_3 nanowires, Appl. Phys. Lett. 84 (2005) 233101.
[38] C. Xiangfeng, W. Caihong, J. Dongli, Z. Chenmou, Ethanol sensor based on indium oxide nanowires prepared by carbothermal reduction method, Chem. Phys. Lett. 399 (2004) 461–464.
[39] J. Liu, X. Wang, Q. Peng, Y. Li, Vanadium pentoxide nanobelts: highly selective and stable ethanol sensor materials, Adv. Mater. 17 (2005) 764–767.

Biographies

Nguyen Van Hieu received his MSc degree from the International Training Institute for Material Science (ITIMS), Hanoi University of Technology (HUT) in 1997 and PhD degree from the Department of Electrical Engineering, University of Twente, Netherlands in 2004. Since 2004, he has been a research lecturer at the ITIMS. In 2007, he worked as a post-doctoral fellow, Korea University. His current research interests include the nano-architectures of carbon nanotubes, oxide semiconductors and oxide semiconductor nanowires for chemical sensors.

Hae-Ryong Kim studied materials science and engineering and received his BS and MS degrees from Korea University in 2005 and 2007, respectively. He is currently a doctoral course candidate at Korea University. His research topic is the preparation of sensor materials via sol–gel routes.

Byeong-Kwon Ju received his ME degree from University of Seoul in 1988. He received his PhD degree from the Department of Electronic Engineering, Korea University in 1995. He joined the Korea Institute of Science and Technology from 1995 to 2005. Since 2005, he is a professor of the Department of Electrical Engineering, Korea University. His current research interests include the application of carbon nanotubes to sensor, MEMS, and nanotechnology.

Jong-Heun Lee has been an Associate Professor at Korea University since 2003. He received his BS, MS, and PhD degree from Seoul National University in 1987, 1989, and 1993, respectively. He has developed automotive air-fuel-ratio sensors at Samsung Advanced Institute of Technology over a 7-year period. His current research interests include chemical sensors, solid electrolyte and functional electroceramics.